

FIG. 1. Expression construct used for the generation of PG-1 transgenic mice. (A) The expression fragment is released from the recombinant mammalian vector pcDNA3-PG-1-His by NruI and PvuII. The full sequence of porcine PG-1-His cDNA was located between the CMV promoter and the BGH polyA tail. (B) Schematic illustration of the precursor PG-1 peptide after intron splicing. It contains a signal peptide that can be released by signal peptidase. The cathelin domain is cleaved by elastase. Upon the removal of these two pieces, the mature PG-1 is the active form of the antimicrobial peptide.

site of the mammalian expression vector pcDNA3 (Invitrogen) between the 645-bp human cytomegalovirus (CMV) immediate-early promoter at the 5' end and a 372-bp bovine growth hormone polyadenylation site (BGH polyA) at the 3' end. The expression cassette was released from the vector with NruI and PvuII, generating a final 1,551-bp DNA expression construct that contained the CMV promoter PG-1-His transgene and the BGH polyA sequences (Fig. 1). PG-1 transgenic mice were generated at the London Transgenic and Gene Targeting Facility (London, Ontario, Canada). Briefly, the PG-1 expression construct was microinjected into pronuclei of fertilized (C57BL/6 × CBA F<sub>1</sub> hybrid) mouse oocytes that were allowed to develop to term after they were transferred to a foster mother. Tail snip samples were collected from the offspring, and PCR was performed to identify animals transgenic for PG-1.

**Real-time RT-PCR.** RNA from both transgenic and wild-type (WT) mouse lung samples were analyzed for PG-1 mRNA transcripts by real-time RT-PCR. The primers used for transgene amplification were as follows: PG-1 forward primer, 5'-GAGCAGTCTCGGAAGCTAA-3'; PG-1 reverse primer, 5'-GTGACTGTCCCCACACTG-3'. The size of the expected PCR amplicon was 201 bp. PCR amplification was conducted on a SmartCycler instrument (Cepheid, Sunnyvale, CA) with the following parameters: 95°C for 15 s, 54°C for 30 s, and 72°C for 30 s for a total of 40 cycles, with a final cycle of 72°C for 30 s. To confirm the cDNA quality and quantity, parallel reactions were carried out with RNA polymerase II-specific primers (as a housekeeping control gene), with 5'-GGTGGAGAGGATGGACAA-3' used as the forward primer and 5'-GCCCAACACAAAACACTCT-3' used as the reverse primer. A reaction without reverse transcriptase (Moloney murine leukemia virus; Invitrogen) was included as a control for DNA contamination. For each set of primers, the cDNA was replaced with water in one reaction to rule out potential contamination. The specificity of the RT-PCR was determined by melting curve analyses, and the products amplified were further verified by agarose gel electrophoresis and DNA sequencing.

**Western blot analysis.** Aliquots of lung tissue (~50 mg) were processed for protein extraction and were evaluated by Western blot analysis, as described previously (5). Protein samples (45 µg) were resolved on 12% sodium dodecyl sulfate-polyacrylamide gels and transferred onto Immobilon polyvinylidene difluoride membranes (Millipore, Bedford, MA). After the membranes were blocked, they were incubated with rabbit monoclonal anti-His tag antibody (1:500; Cell Signaling Technology, Beverly, MA) and then anti-rabbit immunoglobulin G horseradish peroxidase-linked antibody (1:1,000; Cell Signaling Technology). Detection was carried out with an ECL Plus Western blotting detection system (Amersham, Piscataway, NJ), the blots were exposed to X-ray scientific imaging films (Konica, Mexico), and the films were developed with an SRX-101A film processor (Konica, Mexico). To verify that equal amounts of proteins were loaded in each lane, the membranes were stripped and reincubated with primary anti-GAPDH antibody (1:20,000; Abcam, Cambridge, MA) and then anti-mouse immunoglobulin G horseradish peroxidase, and visualization was performed as described above.

**Bacterial preparation.** The O2A *S. suis* strain 96-2247, used in the current study, has been characterized previously (23). A lyophilized *A. suis* stock was liberally

streaked onto sheep blood agar plates (BAPs; Fisher Scientific, Ottawa, Ontario, Canada) and incubated overnight at 37°C in an atmosphere of 5% CO<sub>2</sub>. A single hemolytic colony was then selected and liberally streaked on BAPs and incubated as described above. Bacteria were aseptically harvested in 5 ml of sterile phosphate-buffered saline (PBS; pH 7.4), pelleted by centrifugation at 4,500 × g for 15 min, and then resuspended in ~2 ml of PBS. The cell suspensions were adjusted to an optical density at 600 nm of 0.6 to give a final concentration of approximately 5 × 10<sup>8</sup> CFU/ml (range, 3.5 × 10<sup>8</sup> to 5.9 × 10<sup>8</sup> CFU/ml). The precise counts were determined by plating 10-fold serial dilutions onto BAPs.

**Respiratory infection and postmortem analysis.** Transgenic mice that expressed PG-1 (identified by PCR, RT-PCR, and Western blot analysis) and their WT littermates were denoted the transgenic and the WT groups, respectively. Transgenic, PG-1-nonexpressing mice were excluded from the experiments. Progeny from both the F<sub>1</sub> and the F<sub>2</sub> generations were used in the study. Transgenic (*n* = 68) and WT (*n* = 58) mice that were 6 to 7 weeks old and that weighed 18 to 22 g were used for experimental infection. Serological testing showed that all animals were free of the usual viral and bacterial pathogens and were housed in Horsfal units in a temperature-controlled environment with 12-h light/12-h dark cycle and free access to food and water. After a 6-day acclimation period, the mice were anesthetized with halothane-oxygen and inoculated intranasally with 30 µl of the bacterial suspensions. The mice were monitored for clinical signs every 6 h for the first 48 h postinoculation and at least three times per day until the end of the experiment. A score of 1 was given for any of the following clinical signs: ruffled hair coat, hunched posture, or marked lethargy. A score of 2 was given for nasal discharge, sunken eyes, labored breathing, or wasp waist. The total scores for each clinical observation period for each day (maximum score, 10) were averaged to generate an overall daily clinical score for each group. Mice with a total score of 8 or higher for three consecutive observations were humanely euthanized by CO<sub>2</sub> inhalation and necropsied. All remaining mice were euthanized 6 days after inoculation.

**Measurement of bacterial load.** At necropsy, lung tissue (approximately 20 to 35 mg) was placed in a preweighed sterile 1.5-ml tube. The weights were recorded, and all lung samples were immediately homogenized with a high-speed tissue homogenizer (Fisher Scientific). To facilitate homogenization, 100 µl of sterile PBS was added to each lung tissue sample. The resulting tissue homogenate (~100 µl) was spread on BAPs, and the BAPs were incubated overnight at 37°C in an atmosphere of 5% CO<sub>2</sub>. Only bacteria showing the characteristic *A. suis* phenotype were enumerated.

**Microscopic evaluation of lung tissue.** The right lung of each challenged mouse was used for histologic evaluation. It was gently instilled with 10% buffered formalin, immersed in the same solution for fixation before it was embedded in paraffin, sectioning, and staining with hematoxylin-eosin for microscopic examination. The slides were scored by a pathologist who was unaware of the experimental treatments. To quantitatively compare the severity of the lesions, the lungs were scored for edema, hemorrhage, leukocyte infiltrate, and necrosis according to the system shown in Table 1. A maximum score of 15 was possible for the most severely affected tissues.

TABLE 1. System used to score the different pathology types

Pathology type	Score	Scoring criteria
Edema	0	Normal appearance
	1	Minimal focal perivascular or interstitial
	2	Mild focal perivascular or interstitial
	3	Moderate focal to locally extensive, perivascular, and interstitial
Hemorrhage	0	None
	1	Mild (focal)
	2	Moderate with up to 25% section affected, mild/focal or locally extensive
	3	Marked with a >25% section affected, focal to locally extensive
Infiltrate	0	None
	1	Minimal with less than three vessels affected, up to three layers of cells surrounding
	2	Mild with 3 to 10 vessels, up to three layers, no interstitial infiltrates
	3	Moderate with 10 or more vessels, three layers or more, focal/patchy interstitial
Necrosis	0	None
	2	Mild with focal necrosis and a <10% section affected
	3	Moderate with mild/focal to locally extensive, >10% to 25% affected
	4	Marked with focal to locally extensive, >25% affected, large areas of consolidation

**Neutrophil secretion collection.** Peripheral blood neutrophils were isolated as described previously (31). Freshly isolated neutrophils were washed once in PBS and resuspended at  $10^8$  cells/ml in PBS containing 1 mM  $\text{Ca}^{2+}$  and 1 mM  $\text{Mg}^{2+}$  for degranulation. The neutrophils were then incubated with 100 ng/ml of phorbol 12-myristate 13-acetate (Sigma-Aldrich, St. Louis, MO) at 37°C for 30 min to stimulate secretion. The neutrophil secretions in the supernatant were collected after removal of the neutrophils by centrifugation at  $13,000 \times g$  for 1 min and were then stored at  $-80^\circ\text{C}$  until use.

**RDA.** A radial diffusion assay (RDA) was conducted to detect the activities of the antimicrobial peptides, as described previously (18), by using *Escherichia coli* DH5 $\alpha$  ( $\sim 4 \times 10^7$  CFU/ml) as the test bacterium. Aliquots (10  $\mu\text{l}$ ) of each of the test samples were added to individual wells. Following incubation at 37°C for 16 to 24 h, the diameter of the clear zone of growth inhibition was measured. Antimicrobial activities were expressed in units (0.1 mm = 1 U), calculated by subtracting the diameter of the well from the diameter of the clear zone. The final radial diffusion unit was corrected by the concentration of neutrophils used.

**BALF collection and cytospin preparation.** Mice ( $n = 29$ ) were challenged for 16 h as described above, and cells were recovered by bronchoalveolar lavage (28). One milliliter of the bronchoalveolar lavage fluid (BALF) was immediately diluted (1:1) with PBS and centrifuged at  $1,000 \times g$  for 10 min to pellet the cells. Total cell counts were determined with a hemacytometer. A cytocentrifuge technique was used to prepare BALF cytology specimens stained with May-Grünwald Giemsa stain, as described previously (15, 16). A minimum of 200 cells was counted for each slide prepared, and differential cell counts were determined by a veterinary diagnostician who was unaware of the experimental treatments.

**Validations of in vitro production, secretion, and functionality of PG-1.** Transgenic and WT littermates were euthanized at 4 to 5 weeks of age by  $\text{CO}_2$  inhalation, and tissues were collected for fibroblast isolation. The isolation procedures, culture conditions, and media have been described previously (41). Twenty-four hours before sample collection, the culture medium was replaced with 5 ml of serum- and antibiotic-free medium to avoid interference with subsequent antimicrobial activity determination. To cleave the proform of PG-1

into the mature form of PG-1, the tissue samples were digested with 100  $\mu\text{g}/\text{ml}$  human neutrophil elastase (Elastin Product Company, Owensville, MO) at 37°C for 1 h. All samples were evaluated for the PG-1-His protein by Western blot analyses, and antimicrobial activity was measured by RDAs.

**Statistical analysis.** The results are expressed as the means  $\pm$  standard errors of the means (SEMs) for two to six independent experiments. Analysis of variance was used for between-group comparisons, followed by Tukey's test or Dunnett's post-hoc test (where applicable) with GraphPad Prism (version 3.03) software (San Diego, CA). A  $P$  value of  $<0.05$  was considered significant.

## RESULTS

**Generation and characterization of PG-1 expression in transgenic mice.** Of the 45 offspring ( $F_0$ ) produced following DNA microinjection of the PG-1 construct (Fig. 1), 4 were identified as transgenic by PCR with PG-1-specific primers (data not shown).  $F_1$  and  $F_2$  heterozygotes were generated by breeding with WT mice. No significant differences in growth, behavioral performance, or mean body weight (transgenic mice,  $19.95 \pm 0.4$  g; WT mice,  $19.45 \pm 0.3$  g;  $P > 0.05$ ) were observed between the PG-1 transgenic mice and their WT littermates. As shown in Fig. 2A, PG-1 mRNA was detected in the lung tissue of transgenic mice by real-time RT-PCR. As well, the predicted 17-kDa His-tagged PG-1 protein was detected in the lungs of these transgenic mice by Western blotting with polyclonal anti-His antibody (Fig. 2B). As expected, the PG-1 protein was not detected in the lung tissues of WT mice. The transgenic PG-1-expressing mice were designated the "transgenic group," while their WT littermates were used as negative controls; transgenic mice that did not express PG-1 were excluded from the experiments.

**PG-1 transgenic mice are more resistant to intranasal challenge with *A. suis*.** To determine if the ectopic expression of PG-1 increased the host defense against bacterial infection, PG-1 transgenic mice and their WT littermates were inoculated with 30  $\mu\text{l}$  of *A. suis* ( $1.0 \times 10^8$  to  $5.9 \times 10^8$  CFU/ml)

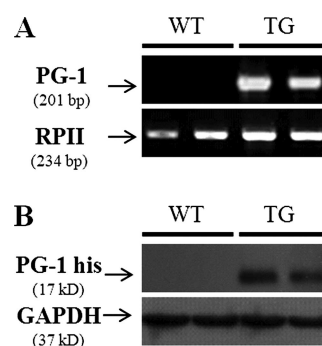


FIG. 2. Expression of PG-1 in the lungs of mice. (A) Representative gel image of RT-PCR results. Total RNA was isolated from the lungs of WT and transgenic (TG) mice, and RT-PCR was conducted with PG-1-specific primers. The PCR products were resolved on a 1% agarose gel and stained with ethidium bromide for visualization. No PG-1 transcript was detected in WT mouse lung tissue, while a clear 201-bp band could be visualized in transgenic mouse lung tissue samples. Amplification of RNA polymerase II (RPII) was used as a loading control. (B) Representative Western blot showing the expression of PG-1-His in transgenic mouse lung tissue. Proteins were extracted from the lungs of WT and transgenic mice, separated by sodium dodecyl sulfate-polyacrylamide gel electrophoresis, and immunoblotted with anti-His tag antibody. The housekeeping protein GAPDH was used as the loading control.

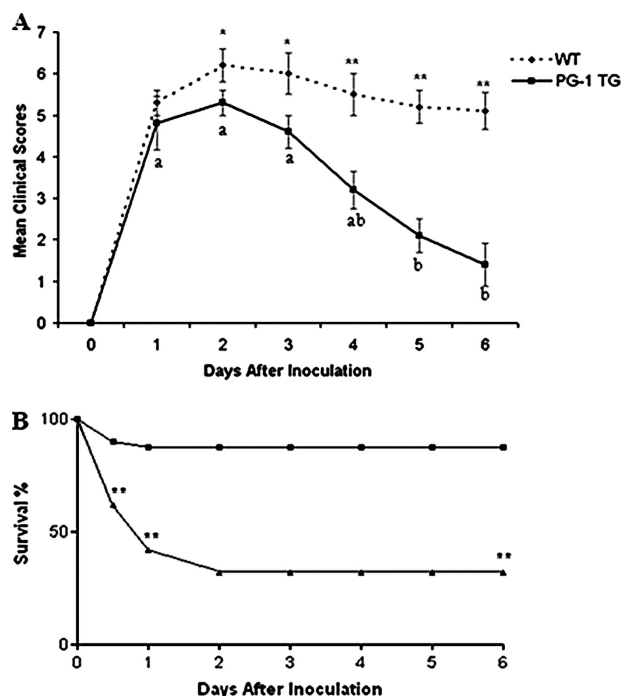


FIG. 3. Comparison of clinical scores (A) and survival rates (B) of PG-1 transgenic (TG) mice and their WT littermates after intranasal inoculation of *A. suis*. The day of inoculation is indicated as day 0. Data represent the means  $\pm$  SEMs of six independent experiments (transgenic mice,  $n = 68$ ; WT mice,  $n = 58$ ). Asterisks indicate a significant difference between the two groups for each day at significance levels of  $P < 0.05$  (\*) and  $P < 0.01$  (\*\*). Different superscripts indicate significant differences between the mean clinical scores within the transgenic group during the 6-day experiment ( $P < 0.05$ ). The mean clinical scores within the WT group were not significantly different ( $P > 0.05$ ).

intranasally. Following challenge, the signs most commonly observed were ruffled hair coat, dyspnea, and lethargy. The average clinical scores were not significantly different between the transgenic mice ( $4.85 \pm 0.4$ ) and the WT mice ( $5.26 \pm 0.3$ ) for the first 24 h after bacterial challenge. On day 2 postinoculation and thereafter, the clinical scores were significantly lower in the transgenic mice than in their WT littermates (Fig. 3A). In the PG-1 transgenic group, the average clinical scores were significantly decreased by day 5 postinoculation compared to those at day 1 postinoculation, suggesting a significant recovery from the infection in this group. As shown in Fig. 3B, mortality or the early removal of animals from the study based on severe clinical signs occurred on days 1 and 2. No further mortality was observed in either group after 48 h postinoculation. Of the 58 WT mice challenged, 31% survived to day 6, while 87.5% of the 68 transgenic mice survived the infection. The difference in survival rates was statistically significant ( $P < 0.01$ ). No clinical signs were observed in control mice inoculated with sterile PBS.

**Reduced severity of microscopic changes in PG-1 transgenic mice.** Representative lungs from PBS-inoculated control mice, transgenic PG-1-expressing mice, and the WT littermates removed on day 6 after inoculation with *A. suis* are shown in Fig. 4A. The pulmonary changes induced in PG-1 transgenic mice following inoculation with *A. suis* included moderate intersti-

tial and alveolar edema with mild, mixed leukocytic infiltrates (Fig. 4A, panels d to f). In contrast, the overall microscopic appearance of the lungs from WT mice were characterized by acute alveolar and interstitial edema, patchy hemorrhage, and marked alveolar and interstitial mixed leukocytic infiltrates (Fig. 4A, panels g to i). In addition, there was multifocal degeneration of the bronchiolar epithelium in the lungs of WT mice, with scattered discrete colonies of intact bacteria (Fig. 4A, panels g to i). The microscopic scores are summarized in Fig. 4B. Scores for hemorrhage ( $P < 0.01$ ), leukocytic infiltrates ( $P < 0.05$ ), and necrosis ( $P < 0.05$ ) were significantly higher in the WT group than in the transgenic group (Fig. 4B).

**Pulmonary clearance of bacteria.** To determine if the histopathological and clinical scores following *A. suis* infection in PG-1 transgenic mice were related to the pulmonary bacterial load, the lungs of the challenged mice were removed on day 6 postinoculation. Representative bacterial cultures of lung tissue homogenates of the transgenic and WT mice are shown in Fig. 5A and B, respectively. Over 90% of the colonies had a morphology typical of that of *A. suis*. The number of *A. suis* CFU recovered from the PG-1 transgenic mice was significantly lower ( $P < 0.01$ ) than that recovered from the WT littermates (Fig. 5C). The numbers shown in Fig. 5C are likely an underestimation of the difference between the two groups, as the lung tissue samples from the nonsurviving animals were excluded from the analysis and twice as many WT mice were removed before day 6 postinoculation.

**PG-1 produced by transgenic animals was functional.** To confirm that PG-1 transgenic mice were capable of producing biologically active PG-1, the antimicrobial activities of neutrophil secretions were examined in RDAs. The bactericidal activity in the medium with stimulated neutrophils from transgenic mice was twofold that of their nontransgenic littermates (Fig. 6A). As it is known that neutrophils contain multiple antibacterial components (12), the antimicrobial activity detected in the WT littermate group likely reflects the basal activity of these factors. To further confirm the PG-1-specific antimicrobial activity of the cells from the PG-1 transgenic mice, fibroblasts, which do not naturally possess antimicrobial activity, were isolated from the mice. These cells were cultured in antibiotic-free medium for 24 h prior to the collection of cell pellets and secretion in the medium. Western blot analysis revealed the presence of PG-1 in both the cells and the culture medium of transgenic fibroblasts (Fig. 6B). To further assess the antimicrobial activity, an RDA was conducted. When the proteins secreted in the medium were treated with neutrophil elastase, a clear antibacterial zone was seen by RDA (Fig. 6C, quadrant 5); no activity was observed without neutrophil elastase treatment (Fig. 6C, quadrant 6). A similar result was seen after PG-1-His was purified with a MAGNEHis protein purification system (Fig. 6C, quadrants 7 and 8). An antibacterial zone was also evident for the transgenic fibroblast cellular protein after elastase treatment (Fig. 6C, quadrants 9 and 10). No antimicrobial activity was detected in fibroblasts to the spent culture medium with fibroblasts from the WT littermate group, regardless of the neutrophil elastase treatment (Fig. 6C, quadrants 11 to 14).

**Differential cell count in BALF.** To investigate the possible association of PG-1 expression with the inflammatory response to bacterial infection, BALF was collected from transgenic and

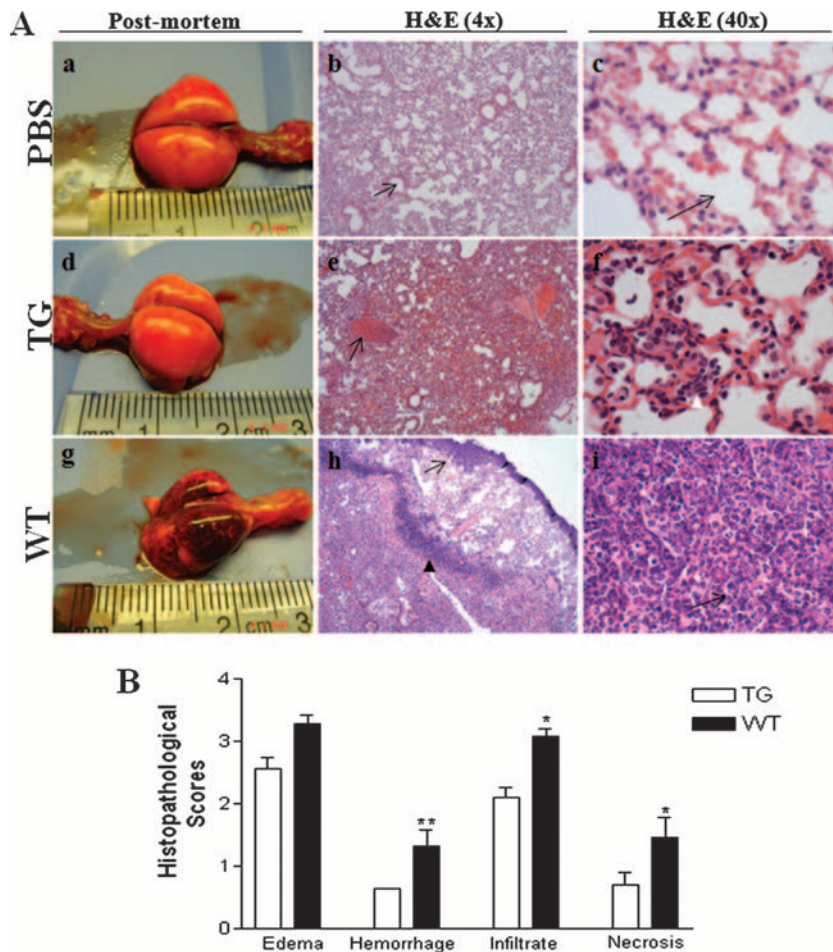


FIG. 4. Comparison of gross and microscopic pulmonary injury after inoculation of *A. suis*. (A) Representative photographs of the gross appearance of whole lungs of mice inoculated with PBS (a), PG-1 transgenic (TG) mice inoculated with *A. suis* (d), and the WT littermate mice inoculated with *A. suis* (g) at postmortem examination. Tissue sections from mice inoculated with PBS were normal, with no evidence of edema, hemorrhage, leukocytic infiltrates, or necrosis; and the alveolar spaces were clear (b and c; arrows). Tissue sections from transgenic mice inoculated with *A. suis* showed focal congestion (e; arrow) and moderate neutrophilic infiltrates (f; white arrowhead). Tissue sections from WT mice inoculated with *A. suis* showed marked congestion (h; arrow), intact bacteria (h; black arrowhead), and marked neutrophilic and macrophage infiltrates within the alveolar spaces (i; arrow). H&E, hematoxylin-eosin. (B) Overall histopathological score (Table 1) for lungs from transgenic mice (open bars) and WT mice (solid bars) inoculated with *A. suis*. Data represent the means  $\pm$  SEMs (PBS-inoculated mice,  $n = 6$ ; transgenic mice,  $n = 33$ ; WT mice,  $n = 24$ ). \*\*,  $P < 0.01$ ; \*,  $P < 0.05$ .

WT mice, and a differential leukocytic cell count was done. No significant difference was observed in total cell counts (transgenic mice,  $0.41 \times 10^6 \pm 0.8 \times 10^6/\text{ml}$ ; WT mice,  $0.31 \times 10^6 \pm 0.1 \times 10^6/\text{ml}$ ) or the numbers of lymphocytes or macrophages isolated in BALF obtained from the challenged transgenic and WT mice (Fig. 7). However, the neutrophil count was almost threefold higher in the BALF from challenged transgenic mice than in the BALF from their WT littermates ( $P < 0.001$ ). There was no significant difference in BALF cell counts from transgenic and WT mice inoculated with PBS (data not shown).

## DISCUSSION

The current study demonstrated that a porcine-specific antimicrobial peptide-encoding gene introduced into the mouse genome via the transgenic approach can be transcribed, translated, and secreted and is functional both in vitro and in vivo.

PG-1 transgenic mice have enhanced resistance to experimental bacterial infection, as evidenced by a significant decrease in the pulmonary bacterial burden, a reduced severity of clinical signs, and higher survival rates after *A. suis* intranasal challenge compared to those for their WT littermates.

PG-1 possesses its own signal peptide-encoding sequence at the 5' end of its mRNA (40), which, after being translated, directs the secretion of the proform of PG-1 (the cathelin-like domain encoded by the proform sequence, together with the active form of PG-1) in neutrophils. Our finding that the PG-1 protein could be detected in the medium after transgenic fibroblast culture indicates that this neutrophil-derived signal peptide is capable of directing protein secretion in other somatic cells. In addition, it is known that only the mature C-terminal portion of PG-1 possesses antimicrobial activity after it is cleaved from the proform by neutrophil elastase (6). In the current study, we chose to express the proform of PG-1 as the

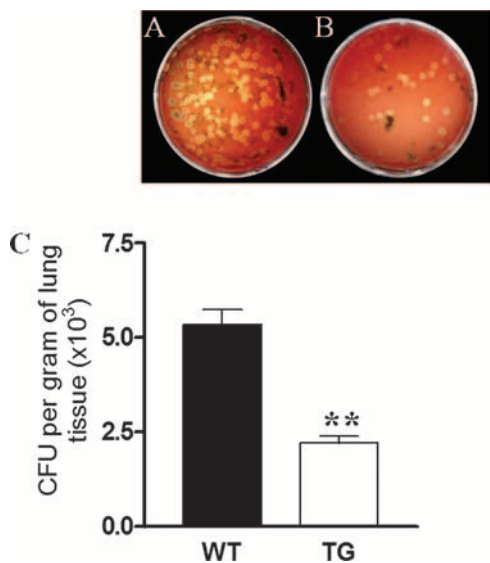


FIG. 5. Bacterial recovery from the lungs of challenged mice. Representative cultures of *A. suis* colonies recovered from homogenized lungs of WT mice (A) and transgenic (TG) mice (B) 6 days after bacterial challenge; (C) quantitation of *A. suis* CFU enumerated on BAPs ( $P < 0.01$ ). Data represent the means  $\pm$  SEMs of six independent experiments (transgenic mice,  $n = 62$ ; WT mice,  $n = 29$ ). \*\*,  $P < 0.01$ .

primary transgene product. This was done to minimize the possible cytotoxic effects that mature PG-1 may have on mammalian somatic cells that are constantly exposed to the antimicrobial peptide. All the transgenic founders and progeny were

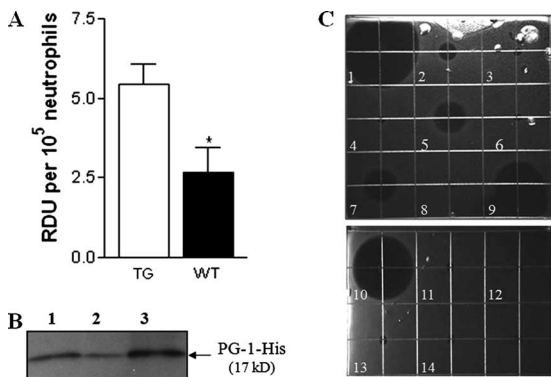


FIG. 6. Bactericidal activity of protein isolated from PG-1 transgenic and WT mice. (A) Bactericidal activity of neutrophil secretions isolated from the blood of transgenic (TG) mice ( $n = 8$ ) and WT mice ( $n = 9$ ) (RDU, radial diffusion unit). (B) Representative Western blot showing the PG-1-His protein in the medium of transgenic fibroblast culture after (lane 1) and before (lane 2) His purification and in transgenic fibroblast cell pellets (lane 3). (C) Representative results of an RDA: quadrants 1 and 10, ampicillin 100  $\mu$ g/ml; quadrant 2, WT neutrophil secretion; quadrant 3, resuspension buffer of sample purification; quadrant 4, neutrophil elastase; quadrants 5 and 6, unpurified medium of cultured transgenic fibroblast medium digested with (quadrant 5) or without (quadrant 6) without neutrophil elastase; quadrants 7 and 8, His-purified medium of cultured transgenic fibroblast digested with (quadrant 7) or without (quadrant 8) neutrophil elastase; quadrants 9 and 10, transgenic fibroblast cell pellet digested with neutrophil elastase; quadrants 11 and 12, medium of cultured WT fibroblast medium digested with (quadrant 11) or without (quadrant 12) neutrophil elastase; quadrants 13 and 14, WT fibroblast cell pellet digested with (quadrant 13) or without (quadrant 14) neutrophil elastase.

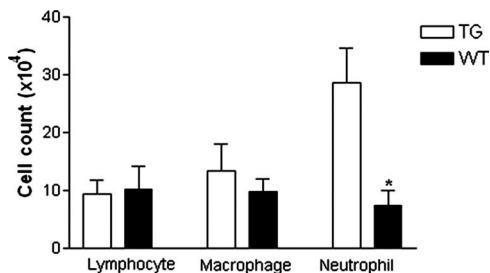


FIG. 7. Differential cell counts from BALF. Transgenic (TG) and WT mice were challenged with *A. suis* and euthanized 16 h postinoculation. BALF was collected, cytocentrifuged, and stained with May-Grünwald Giemsa. Data represent the means  $\pm$  SEMs from two independent experiments (transgenic mice,  $n = 9$ ; WT mice,  $n = 10$ ). \*,  $P < 0.05$ .

fertile and healthy, a with growth rate similar to that of the WT littermates, suggesting that there were no adverse effects related to ectopic transgene overexpression. Similar infection-resistant results were observed for progeny produced by another independent PG-1 transgenic line (data not shown), suggesting that a major genome disruption effect is unlikely. In addition, the findings that the antimicrobial activity in neutrophil secretions was significantly higher and that the bacterial burden in the lungs of challenged mice was lower than those in the transgenic group together suggest that the proform of PG-1 was appropriately cleaved in murine neutrophils and at the site of infection in the lungs. The improved clinical outcome and decreased pulmonary bacterial burden in inoculated transgenic mice suggested that PG-1 has significant antimicrobial activity in vivo. Previous studies have shown that elastase activity was detected in the respiratory tract and increased during infection and inflammation (29). It is conceivable that the proform of PG-1 produced in the lung was proteolytically cleaved by elastase from neutrophils that had migrated to the site of infection and that the mature form of PG-1 released exerted an antimicrobial function in vivo.

Early studies suggested that the ectopic expression of antimicrobial peptides can combat a pathogenic infection (36). In addition to the potent bactericidal capability of PG-1, it is possible that PG-1 acts in synergy with other locally produced host defense peptides to more effectively overcome pathogen invasion. A previous study examined the possible synergistic activities of several important defense peptides, including PG-1, LL-37, bovine bactenecin, and indolicidin; PG-1 was found to have the highest synergistic bactericidal activity against almost all bacteria tested (39). Nevertheless, emerging evidence suggests that the functions of antimicrobial peptides are not solely limited to bacterial killing. It is believed that these small peptides may also exert broader functions as an integral part of the innate immune system, exerting either immunostimulating or immunomodulating effects (4, 13, 37). Most of the studies examining the immunomodulatory function of members of the cathelicidin family so far have been focused on the human cathelicidin peptide LL-37. The role of LL-37 appears to be both proinflammatory and anti-inflammatory. For example, LL-37 stimulates cytokine and chemokine secretion by monocytes in vitro (3) and provides a chemotactic function for monocytes, neutrophils, and mast cells

(2, 22, 35). The role of PG-1 on the host immune response is currently unclear. In our study, the numbers of neutrophils in BALF was threefold higher in the transgenic mice than in their nontransgenic littermates at 16 h after challenge. At an early stage of infection, neutrophils may migrate to the site of infection to enhance the host defense via phagocytosis and direct pathogen killing. It is possible that one of the mechanisms by which the reduced lesion severity and improved survival of transgenic mice occurs in response to bacterial challenge is through the chemotactic signaling of PG-1. This may promote the early migration of neutrophils to the site of infection, reducing bacterial colonization and subsequent tissue damage. It has been shown that LL-37 utilizes formyl peptide receptor-like 1, a chemotactic receptor that binds to multiple endogenous and bacterium-derived ligands, to chemoattract neutrophils (8). Whether PG-1 recruits neutrophils via a similar mechanism is currently unknown. In addition, it was recently reported that PG-1 acts as an effective inducer, promoting the release of interleukin-1 beta through posttranslational processing and thus facilitating the proinflammatory response (26). Future experiments are aimed at the further identification of the factors and mechanisms involved in the PG-1-mediated host immune response. It will be particularly interesting to determine whether it is the PG-1 cathelin domain or the full-length PG-1 that possesses this function.

The current study demonstrates that the transgenic expression of PG-1 in mice confers enhanced resistance to experimental bacterial infection. It provides a proof-of-principle basis for the development of transgenic pigs that ectopically express PG-1 in other somatic tissues beyond neutrophils. To further eliminate the possibility of microbial resistance development due to its constitutive expression, future studies may utilize a specific promoter so that the expression of the antimicrobial peptide can be temporally and spatially controlled. For example, an inducible promoter such as the tracheal antimicrobial peptide promoter could be employed to direct the expression of the peptide primarily in respiratory epithelial cells only and upon bacterial stimulation (9, 10). Moreover, recent studies suggest that the xenobiotic expression of antimicrobial peptides is highly beneficial to the transgenic host defense (17, 30). As PG-1 is known to be expressed only in the pig, the xenobiotic expression of PG-1 in other animals may allow the development of lines of livestock that potentially have superior resistance to a various microbial infections. Since mice do not naturally harbor the PG-1 gene, the transgenic mice generated in the study thus also provide a valuable model for studying the role and mechanism of action of this antimicrobial peptide *in vivo*.

#### ACKNOWLEDGMENTS

Financial support for this work was provided by Ontario Pork, the Natural Sciences and Engineering Council of Canada, and the Ontario Ministry of Agriculture and Food and Rural Affairs.

We thank Perrin Baker, Lihua Wen, Sarah Armstrong, and Shella Watson for excellent technical assistance. We also thank Shivani Ojha for help with the bacterial challenge protocol and sharing information prior to publication. We recognize the technical assistance provided by the staff at the Central Animal Facility and Isolation Units at the University of Guelph.

De Wu is a visiting scholar from the Institute of Animal Nutrition, Sichuan Agricultural University, China.

#### REFERENCES

- Benincasa, M., M. Scocchi, S. Pacor, A. Tossi, D. Nobili, G. Basaglia, M. Busetti, and R. Gennaro. 2006. Fungicidal activity of five cathelicidin peptides against clinically isolated yeasts. *J. Antimicrob. Chemother.* **58**:950–959.
- Bowdish, D. M., D. J. Davidson, M. G. Scott, and R. E. Hancock. 2005. Immunomodulatory activities of small host defense peptides. *Antimicrob. Agents Chemother.* **49**:1727–1732.
- Bowdish, D. M., D. J. Davidson, D. P. Speert, and R. E. Hancock. 2004. The human cationic peptide LL-37 induces activation of the extracellular signal-regulated kinase and p38 kinase pathways in primary human monocytes. *J. Immunol.* **172**:3758–3765.
- Braff, M. H., M. A. Hawkins, A. Di Nardo, B. Lopez-Garcia, M. D. Howell, C. Wong, K. Lin, J. E. Streib, R. Dorschner, D. Y. Leung, and R. L. Gallo. 2005. Structure-function relationships among human cathelicidin peptides: dissociation of antimicrobial properties from host immunostimulatory activities. *J. Immunol.* **174**:4271–4278.
- Burnette, W. N. 1981. "Western blotting": electrophoretic transfer of proteins from sodium dodecyl sulfate-polyacrylamide gels to unmodified nitrocellulose and radiographic detection with antibody and radioiodinated protein A. *Anal. Biochem.* **112**:195–203.
- Cole, A. M., J. Shi, A. Ceccarelli, Y. H. Kim, A. Park, and T. Ganz. 2001. Inhibition of neutrophil elastase prevents cathelicidin activation and impairs clearance of bacteria from wounds. *Blood* **97**:297–304.
- Confer, A. W. 1993. Immunogens of *Pasteurella*. *Vet. Microbiol.* **37**:353–368.
- De, Y., Q. Chen, A. P. Schmidt, G. M. Anderson, J. M. Wang, J. Wooters, J. J. Oppenheim, and O. Chertov. 2000. LL-37, the neutrophil granule- and epithelial cell-derived cathelicidin, utilizes formyl peptide receptor-like 1 (FPR1) as a receptor to chemoattract human peripheral blood neutrophils, monocytes, and T cells. *J. Exp. Med.* **192**:1069–1074.
- Diamond, G., V. Kaiser, J. Rhodes, J. P. Russell, and C. L. Bevins. 2000. Transcriptional regulation of beta-defensin gene expression in tracheal epithelial cells. *Infect. Immun.* **68**:113–119.
- Dyce, P. W., R. J. DeVries, J. Walton, R. R. Hacker, and J. Li. 2003. Inducible expression of green fluorescent protein in porcine tracheal epithelial cells by the bovine tracheal antimicrobial peptide promoter. *Biotechnol. Bioeng.* **84**:374–381.
- Fattorini, L., R. Gennaro, M. Zanetti, D. Tan, L. Brunori, F. Giannoni, M. Pardini, and G. Orefici. 2004. *In vitro* activity of protegrin-1 and beta-defensin-1, alone and in combination with isoniazid, against *Mycobacterium tuberculosis*. *Peptides* **25**:1075–1077.
- Gudmundsson, G. H., and B. Agerberth. 1999. Neutrophil antibacterial peptides, multifunctional effector molecules in the mammalian immune system. *J. Immunol. Methods* **232**:45–54.
- Hancock, R. E., and H. G. Sahl. 2006. Antimicrobial and host-defense peptides as new anti-infective therapeutic strategies. *Nat. Biotechnol.* **24**:1551–1557.
- Jensen, L. B., A. M. Hammerum, F. Bager, and F. M. Aarestrup. 2002. Streptogramin resistance among *Enterococcus faecium* isolated from production animals in Denmark in 1997. *Microb. Drug Resist.* **8**:369–374.
- Klech, H., and C. Hutter. 1990. Clinical guidelines and indications for bronchoalveolar lavage (BAL): report of the European Society of Pneumology Task Group on BALF. *Eur. Respir. J.* **3**:937–974.
- Lavolette, M., M. Carreau, and R. Coulombe. 1988. Bronchoalveolar lavage cell differential on microscope glass cover: a simple and accurate technique. *Am. Rev. Respir. Dis.* **138**:451–457.
- Lee, P. H., T. Ohtake, M. Zaiou, M. Murakami, J. A. Rudisill, K. H. Lin, and R. L. Gallo. 2005. Expression of an additional cathelicidin antimicrobial peptide protects against bacterial skin infection. *Proc. Natl. Acad. Sci. USA* **102**:3750–3755.
- Lehrer, R. I., M. Rosenman, S. S. Harwig, R. Jackson, and P. Eisenhauer. 1991. Ultrasensitive assays for endogenous antimicrobial polypeptides. *J. Immunol. Methods* **137**:167–173.
- MacInnes, J. I., and R. Desrosiers. 1999. Agents of the "suis-side diseases" of swine: *Actinobacillus suis*, *Haemophilus parasuis*, and *Streptococcus suis*. *Can. J. Vet. Res.* **63**:83–89.
- Mauch, C., and G. Bilkei. 2004. *Actinobacillus suis*, a potential cause of abortion in gilts and low parity sows. *Vet. J.* **168**:186–187.
- Miyakawa, Y., P. Ratnakar, A. G. Rao, M. L. Costello, O. Mathieu-Costello, R. I. Lehrer, and A. Catanzaro. 1996. *In vitro* activity of the antimicrobial peptides human and rabbit defensins and porcine leukocyte protegrin against *Mycobacterium tuberculosis*. *Infect. Immun.* **64**:926–932.
- Niyonsaba, F., K. Iwabuchi, A. Someya, M. Hirata, H. Matsuda, H. Ogawa, and I. Nagaoka. 2002. A cathelicidin family of human antibacterial peptide LL-37 induces mast cell chemotaxis. *Immunology* **106**:20–26.
- Ojha, S., M. A. Hayes, P. V. Turner, and J. I. MacInnes. 2007. An experimental model of *Actinobacillus suis* infection in mice. *Comp. Med.* **57**:340–348.
- Ojha, S., M. Sirois, and J. I. MacInnes. 2005. Identification of *Actinobacillus suis* genes essential for the colonization of the upper respiratory tract of swine. *Infect. Immun.* **73**:7032–7039.

25. Panyutich, A., J. Shi, P. L. Boutz, C. Zhao, and T. Ganz. 1997. Porcine polymorphonuclear leukocytes generate extracellular microbicidal activity by elastase-mediated activation of secreted proprotegrins. *Infect. Immun.* **65**: 978–985.
26. Perregaux, D. G., K. Bhavsar, L. Contillo, J. Shi, and C. A. Gabel. 2002. Antimicrobial peptides initiate IL-1 beta posttranslational processing: a novel role beyond innate immunity. *J. Immunol.* **168**:3024–3032.
27. Qu, X. D., S. S. Harwig, W. M. Shafer, and R. I. Lehrer. 1997. Protegrin structure and activity against *Neisseria gonorrhoeae*. *Infect. Immun.* **65**:636–639.
28. Rennard, S. I., R. Aalbers, E. Bleecker, H. Klech, L. Rosenwasser, D. Olivieri, and Y. Sibille. 1998. Bronchoalveolar lavage: performance, sampling procedure, processing and assessment. *Eur. Respir. J. Suppl.* **26**:13S–15S.
29. Rudolphus, A., J. Stolk, C. van Twisk, C. J. van Noorden, J. H. Dijkman, and J. A. Kramps. 1992. Detection of extracellular neutrophil elastase in hamster lungs after intratracheal instillation of *E. coli* lipopolysaccharide using a fluorogenic, elastase-specific, synthetic substrate. *Am. J. Pathol.* **141**:153–160.
30. Salzman, N. H., D. Ghosh, K. M. Huttner, Y. Paterson, and C. L. Bevins. 2003. Protection against enteric salmonellosis in transgenic mice expressing a human intestinal defensin. *Nature* **422**:522–526.
31. Shi, J., and T. Ganz. 1998. The role of protegrins and other elastase-activated polypeptides in the bactericidal properties of porcine inflammatory fluids. *Infect. Immun.* **66**:3611–3617.
32. Steinberg, D. A., M. A. Hurst, C. A. Fujii, A. H. Kung, J. F. Ho, F. C. Cheng, D. J. Loury, and J. C. Fiddes. 1997. Protegrin-1: a broad-spectrum, rapidly microbicidal peptide with in vivo activity. *Antimicrob. Agents Chemother.* **41**:1738–1742.
33. Steinstraesser, L., B. Tippler, J. Mertens, E. Lamme, H. H. Homann, M. Lehnhardt, O. Wildner, H. U. Steinau, and K. Uberla. 2005. Inhibition of early steps in the lentiviral replication cycle by cathelicidin host defense peptides. *Retrovirology* **2**:2.
34. Tamamura, H., T. Murakami, S. Horiuchi, K. Sugihara, A. Otaka, W. Takada, T. Ibuka, M. Waki, N. Yamamoto, and N. Fujii. 1995. Synthesis of protegrin-related peptides and their antibacterial and anti-human immunodeficiency virus activity. *Chem. Pharm. Bull. (Tokyo)* **43**:853–858.
35. Tjabringa, G. S., D. K. Ninaber, J. W. Drijfhout, K. F. Rabe, and P. S. Hiemstra. 2006. Human cathelicidin LL-37 is a chemoattractant for eosinophils and neutrophils that acts via formyl-peptide receptors. *Int. Arch. Allergy Immunol.* **140**:103–112.
36. Tzou, P., J. M. Reichhart, and B. Lemaitre. 2002. Constitutive expression of a single antimicrobial peptide can restore wild-type resistance to infection in immunodeficient *Drosophila* mutants. *Proc. Natl. Acad. Sci. USA* **99**:2152–2157.
37. van Wetering, S., G. S. Tjabringa, and P. S. Hiemstra. 2005. Interactions between neutrophil-derived antimicrobial peptides and airway epithelial cells. *J. Leukoc. Biol.* **77**:444–450.
38. Wegener, H. C., F. M. Aarestrup, P. Gerner-Smidt, and F. Bager. 1999. Transfer of antibiotic resistant bacteria from animals to man. *Acta Vet. Scand. Suppl.* **92**:51–57.
39. Yan, H., and R. E. Hancock. 2001. Synergistic interactions between mammalian antimicrobial defense peptides. *Antimicrob. Agents Chemother.* **45**: 1558–1560.
40. Zhao, C., T. Ganz, and R. I. Lehrer. 1995. The structure of porcine protegrin genes. *FEBS Lett.* **368**:197–202.
41. Zhu, H., B. Tamot, M. Quinton, J. Walton, R. R. Hacker, and J. Li. 2004. Influence of tissue origins and external microenvironment on porcine foetal fibroblast growth, proliferative life span and genome stability. *Cell Prolif.* **37**:255–266.